Dalton Transactions

Accepted Manuscript

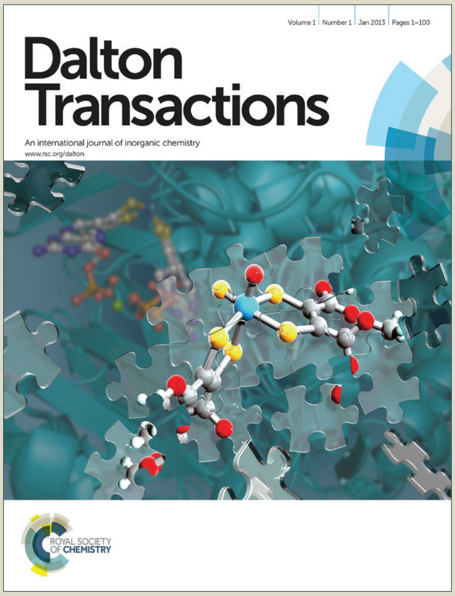

ROYAL SOCIETY OF CHEMISTRY

www.rsc.org/dalton

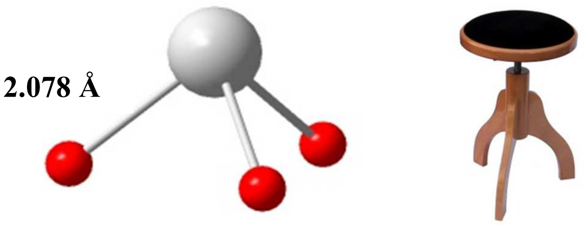

In hyper-alkaline aqueous solutions, the three-legged stool-like $[Sn(OH)_3]^-$ is the only hydroxido complex with very short (2.078 Å) Sn−O distance.

Cite this: DOI: 10.1039/c0xx00000x

www.rsc.org/xxxxxx

ARTICLE TYPE

Speciation and structure of tin(II) in hyper-alkaline aqueous solution

Éva G. Bajnóczi,[a,h] Eszter Czeglédi,[a,h]Ernő Kuzmann,[b] Zoltán Homonnay,[b] Szabolcs Bálint,[c] György Dombi,[d] Péter Forgo,[d] Ottó Berkesi,[e] István Pálinkó,[f,h] Gábor Peintler,[e,h] Pál Sipos,[a,h*] and Ingmar Persson[g*]

Received (in XXX, XXX) XthXXXXXXXXX 20XX, Accepted Xth XXXXXXXXX 20XX

DOI: 10.1039/b000000x

Abstract

The identity of the predominating tin(II)-hydroxide complex formed in hyper-alkaline aqueous solution ($0.2 \leq C_{\mathrm{NaOH}} \leq 12$ mol·dm^{-3}) has been determined by potentiometric titrations, Raman, Mössbauer and XANES spectroscopy, supplemented by quantum chemical calculations. Thermodynamic studies using a H_2/Pt electrode up to free hydroxide concentrations of 1 mol·dm^{-3} showed the presence of a single monomeric complex with a tin(II):hydroxide ratio of 1:3. This observation together with Raman and Mössbauer spectroscopic measurements supplemented by quantum mechanical calculations proved that the predominating complex is $[Sn(OH)_3]^-$, and that the presence of the other possible complex, $[SnO(OH)]^-$, could not be proven with neither experiments nor simulations. The structure of the trihydroxidostannate(II) complex, $[Sn(OH)_3]^-$, was determined by EXAFS and was found to be independent of the applied hydroxide and tin(II) concentrations. The mean Sn-O bond distance is short, 2.078 Å, and in very good agreement with the only structure reported in the solid state. It is also shown that at pH values above 13 the speciation of the predominating trihydroxidostannate(II) complex is not affected by the presence of high concentrations of chloride ions.

Introduction

Under hyper-alkaline conditions (pH > 13) in aqueous systems, many metal ions are able to form mono- and polynuclear hydroxide complexes,[1,2] which in most cases are different from those present in weakly acidic, neutral and weakly alkaline aqueous solution. Crystallization from such solutions often yields solid materials with peculiar local- or nano-structure.[3,4] Knowledge of the structure and dynamics of the solution species formed under these extreme conditions can be the key to understand and control a range of aquatic processes as *e.g.* industrial and geochemical ones.

Hydrolysis of metal ions, composition, structure and thermodynamics of their hydroxido complexes, is one of the classical topics of inorganic solution chemistry. Formation constants for a large variety of hydroxido complexes as well as solubility products of solid metal hydroxides are well known and are collated in various textbooks and data bases.[5,6] Traditionally, species formed in aqueous solution in the pH-range 2-12 are normally well characterized, while the knowledge on the nature of hydroxido-metallate complexes at the extreme alkaline end of the pH scale is scarce due to well-known theoretical as well as practical/technical difficulties. In spite of these hurdles, the number of publications dealing with this particular aspect of solution chemistry steadily increases. For obvious reasons, metal ions with reasonable solubility, *e.g.* amphoteric ones, are most intensely studied including aluminum(III),[7-9] gallium(III),[10,11] chromium(III),[12,13] lead(II)[14] and thallium(I).[15,16] Beside these, data for metal ions that are hardly soluble at alkaline conditions has also emerged as for *e.g.* copper(II),[17] iron(III)[18] and the actinides.[19]

In the current paper, the behaviour of the amphoteric tin(II) ion in hyper-alkaline aqueous media is in focus. The hydrolysis properties of tin(II) in aqueous solution are known with stepwise formation of hydroxido complexes with the formal compositions $[Sn(OH)]^+$, $[Sn(OH)_2]^0$ and $[Sn(OH)_3]^-$ at low metal concentration, while in solutions with higher tin(II) concentration, polynuclear $[Sn_2(OH)_2]^{2+}$ and $[Sn_3(OH)_4]^{2+}$ complexes have been observed as well.[20-22] On the basis of the literature data,[20-22] the last stepwise hydroxido complex formed in aqueous solution with tin(II) has a Sn(II):OH$^-$ ratio of 1:3. No higher complexes have been observed from potentiometric measurements up to 0.25 mol·dm^{-3} free hydroxide concentration.[23] However, it has been claimed that higher complexes as $[Sn(OH)_4]^{2-}$, or even $[Sn(OH)_6]^{4-}$, can possibly be formed under strongly alkaline conditions.[24]

The main objective of the present work is to reveal the identity and structure of the tin(II) complex(es) present in aqueous solution at pH > 13. Systematic potentiometric pH titrations, Raman, Mössbauer and XANES spectroscopic measurements on solutions containing NaOH ($0.1 \leq C_{\mathrm{NaOH}} \leq 12$ mol·dm^{-3}) and tin(II) (0.05 - 0.25 mol·dm^{-3}) together with quantum chemical calculations have been performed to identify the hydroxidostannate(II) complex(es) predominating in hyper-alkaline aqueous solution. The structure of this complex has been revealed by EXAFS. From a practical point of view it is also important to clarify whether or not chloride as counter ion has any effect on the tin(II) speciation at high hydroxide concentration.

Experimental section

Reagents and solutions

Analytical grade sodium hydroxide, NaOH (ANALR NORMAPUR), or potassium hydroxide, KOH (Reanal), was dissolved in distilled water under intensive stirring and cooling to prepare the alkaline stock solutions. The concentration was calculated from the density of the solutions, determined by a picnometer, according to literature procedures.[25] The carbonate content was minimized as described elsewhere.[26] The stock solutions were stored in caustic resistant Pyrex bottles with tightly fitting screw-caps.

The tin(II) containing stock solutions were prepared according to two routes. For the stock solution with $C_{\mathrm{Sn(II)}} \approx 0.5$ mol·dm^{-3} and $C_{\mathrm{acid}} \approx 1$ mol·dm^{-3}, tin(II) oxide powder, SnO (Sigma Aldrich), was dissolved in oxygen-free atmosphere in dilute analytical grade hydrochloric or perchloric acid (Sigma Aldrich). The purity of SnO was checked with powder X-ray diffraction and was found to contain less than *ca.* 2% SnO_2.

The tin(II) stock solution for the potentiometric titrations, $C_{\mathrm{Sn(II)}} \approx 0.6$ mol·dm^{-3} and $C_{\mathrm{HCl}} \approx 1.5$ mol·dm^{-3}, was prepared under oxygen free conditions by dissolving metallic tin (Reanal) in dilute analytical grade hydrochloric acid. This process took about four days and during this time the temperature was kept at 323 K under reflux. A practically tin(IV) free solution could be prepared in this way as the continuously evolving hydrogen gas did secure reducing conditions and any further oxidation of formed tin(II) was not possible. The solution was filtered under nitrogen atmosphere. The exact concentration of tin(II) was determined by the standard iodometric titration procedure, while the concentration of excess hydrochloric acid was determined by pH-potentiometric titration with sodium hydroxide.

The alkaline tin(II) solutions for the X-ray absorption, Raman and ^{119}Sn Mössbauer spectroscopy measurements were prepared in small Pyrex bottles. A custom-made screw-cap was fabricated with two small holes for the argon gas in- and outlet and a larger one for the addition of the tin(II) stock solution. The calculated amount of the freshly prepared tin(II) stock solution was added drop-wise to 25 mL of the appropriately diluted NaOH solution with continuous and intense argon bubbling through the sample and stirring. The NaOH solutions were diluted by weight from the concentrated stock solution, and argon gas was bubbled through it for at least 15 minutes before adding the metal stock solution.

Potentiometric titrations

The pH potentiometric titrations were carried out using a Metrohm 888 Titrando instrument equipped with a H_2/Pt electrode. The experimental protocol used for such measurements have been described in detail elsewhere.[27,28] The electrochemical cell contained a platinized hydrogen electrode and a thermodynamic Ag|AgCl reference electrode.

H^+/H_2(Pt) | test sol., $I = 4$ mol·dm^{-3} (NaCl) ||4 mol·dm^{-3}NaCl ||
4 mol·dm^{-3}NaCl, Ag/AgCl

The behaviour of the electrode was found to be Nernstian, slope: 59.2 ± 0.2 mV/decade. The electrode performance was regularly checked *via* calibrations using strong acid-strong base titrations in the concentration range employed during the measurements. All the titrations were performed in an externally thermostated home-made cell where the temperature was kept at 25.00 ± 0.04 °C by circulating water from a Julabo 12 thermostat. The ionic strength was kept constant, $I = 4$ mol·dm^{-3}, with analytical grade NaCl (Prolabo).

FT-Raman spectroscopy

Raman spectra were recorded on a BIO-RAD Digilab Division dedicated FT-Raman spectrometer equipped with liquid nitrogen cooled germanium detector and CaF_2 beam-splitter. The excitation line was provided by a Spectra Physics T10-106C Nd:YVO_4 laser at 1064 nm. The spectra were recorded in the range 3600 – 100 cm^{-1} with 4 cm^{-1} resolution. 4096 scans were collected and averaged for each spectrum. The excitation power was 280 mW at the sample. The spectrometer was controlled by using BIO-RAD Win IR 3.3 software. The samples were placed in a 1 cm path length quartz cuvette. Spectra were recorded at room-temperature. Data were processed by the SpekWin software[29], and fitting of the Lorentzian curves were performed with QtiPlot.[30] Attempts to collect FT-IR spectra for these solutions in ATR mode were unfortunately unsuccessful, most probably due to insufficient signal-to-noise ratio.

Mössbauer spectroscopy

^{119}Sn Mössbauer spectra of frozen solutions were recorded with a conventional Mössbauer spectrometer (Wissel) in transmission geometry with constant acceleration mode at 78 K in a He-cryostat cooled by liquid nitrogen with the sample kept in He atmosphere. The measurements were carried out using a $Ca^{119m}SnO_3$ radiation source of 8 mCi activity. 20 μm α-Fe was used for velocity calibration when a ^{57}Co/Rh source supplied the γ-rays, and the isomer shifts are given relative to $CaSnO_3$. All sample preparation, including also the rapid freezing, was done in a home-made glove-box to minimize the oxidation of the sample. The Mössbauer spectra were analysed by least-squares fitting of the Lorentzian lines with the help of the MOSSWINN program.[31] The database of the Mössbauer Effect Data Index was used to interpret the results.[32]

NMR spectroscopy

The ^{117}Sn NMR measurements were performed at 178.03 MHz on a 1.75T Bruker Avance NMR spectrometer (500.13 MHz ^{1}H frequency), in 5 mm Wilmad NMR tubes. Other experimental details: solvent: 10% D_2O/90% H_2O, the deuterium signal was used to lock the field; relaxation delay: 1 sec; sweep width: 500.5 ppm; pulse width: 1 μs; temperature: 298.1 K; number of scans: 32.

Computational methods

The complexes studied by computational methods included $[Sn(OH)_3]^-$ and $[SnO(OH)]^-$, and for comparison, $[Sn(H_2O)_3]^{2+}$, $Sn(OH)_2$ and $[SnO(OH)_2]^{2-}$, respectively. Optimizations and frequency analyses were performed using the GAUSSIAN 09 program[33] with density functional theory (DFT) at the B3LYP level, using SDD basis set for tin atoms and 6-31+G** for oxygens and hydrogens.[33] Using more flexible basis sets for the light atoms does not improve the calculated results. The earlier studies of tin complexes proved the suitability of the B3LYP method to calculate the nuclear quadrupole splitting (NQS) of ^{119}Sn.[34-36] The core electron density directly determines the NQS of the tin atom, thus the DGDZVP all electron basis set has been applied for the heavy atom to calculate the NQS with high accuracy. We systematically modelled solvent effects by representing H_2O as a polarizable continuum, according to the method implemented in the PCM-SCRF (self-consistent reaction field) procedure in the Gaussian program. In some cases explicitly the hydration shell of these complexes was taken into account, but the calculated properties did not change significantly compared to the PCM method, therefore, those results are not discussed.

X-ray absorption measurements

The X-ray absorption spectra for tin were collected at the bending magnet beam-line Samba at the Soleil synchrotron facility, Paris, France, which operated at 2.75 GeV and a maximum current of 400 mA. The Samba beam-line covers the energy range 4–42 keV. The maximal flux on the sample at 10 keV was 1×10^{12} photon/s/0.1 % bandwidth. The energy scale of the X-ray absorption spectra were calibrated by assigning the first inflection point of the tin K edges of metallic tin foil to 29200.0 eV.[37] The spectra of the tin(II) solutions were recorded on 15 mL samples placed in a cubic polyethylene sample holder with a tightly fitted screw-cap. The analysis of the data was performed with the EXAFSPAK[38] and FEFF7[37] program packages allowing the determination of the structure parameters of the local coordination around tin(II).

Results and discussion

Potentiometric titrations

In order to establish the composition of the predominating tin(II) complex in hyper-alkaline aqueous solution, the OH^-:tin(II) stoichiometric ratio of the predominating complex was determined by potentiometric pH titrations using an H_2/Pt electrode suitable to work at aqueous hyper-alkaline conditions.[27,28] The total tin(II) and hydroxide concentrations in the titrated solution were 0.1998 and 1.4992 mol·dm^{-3}, respectively.

The titrand was 3.0825 mol·dm^{-3} hydrochloric acid, adjusted to 4 mol·dm^{-3} ionic strength with NaCl. A typical titration curve is shown on Figure 1. The system was inhomogeneous from 7.60 to 20.80 ml of the added hydrochloric acid solution (grey area in Figure 1). The inhomogeneity is caused by the precipitation of $Sn(OH)_2$ and/or hydrated SnO since they have very low solubility in the lack of excess hydroxide. The first equivalence point is close to that point of titration in which the OH^-:tin(II) ratio is 2.0 while the second one corresponds to the complete neutralization of the excess hydroxide. Because of the inhomogeneity, only the initial part of the titration curve (corresponding to titrant consumption < 7.60 mL) can be evaluated. In this range, only the excess NaOH unreacted with tin(II) is neutralized by the added hydrochloric acid. Consequently, the change of the observed cell potential (E) depends on the concentration of the free hydroxide which is determined by the composition of the $[Sn(OH)_x]^{2-x}$ complex. The potential differences between the neighbouring titration points (ΔE) were used for the evaluation were calculated from the Nernst-equation assuming $x = 3$ and 4, respectively. In this way the use of any standard electrode potential (E_o) was not necessary. As it is clearly seen in Figure 1, the calculated ΔE values almost perfectly describe the observed ones for $x = 3$, indicating that the maximum OH^-:tin(II) stoichiometric ratio is strictly, or at least predominantly, 3:1 at hyper alkaline conditions. This means that the formation of $[Sn(OH)_4]^{2-}$ or its dehydrated forms, $[SnO_2]^{2-}$ and $[SnO(OH)_2]^{2-}$, can be excluded to be present in significant concentrations. On the other hand, the formation of $[SnO(OH)]^-$, the dehydrated form of $[Sn(OH)_3]^-$, cannot be distinguished from each other by potentiometry.

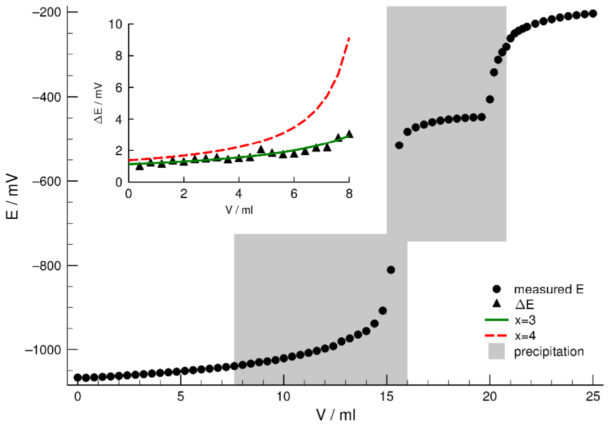

Fig. 1. The potentiometric titration curve of 40 ml solution containing 0.1998 M Sn(II) and 1.4992 M NaOH; titrant: 3.0825 M HCl. The grey area shows the inhomogeneous region of the titration. Insert: the observed and calculated potential differences for $x = 3$ (solid green line) and 4 (dashed red line), where x stands for $[Sn(OH)_x]^{2-x}$.

FT-Raman spectroscopy

Background subtracted FT-Raman spectra of solutions with $C_{NaOH} = 4.0$ mol·mol^{-3} and various amounts of tin(II) are shown in Figure 2. With increasing tin(II) concentration, a spectral feature emerges at ~430 cm^{-1} and another one, less intense, at ~490 cm^{-1}. According to literature data both are assigned to Sn-O vibrations; a broad weak spectral feature is seen in Raman spectra of SnO, $Sn(OH)_2$ and SnO_2 in solid state at ~470 cm^{-1}.[40-42]

The peak at ~580 cm^{-1} in Figure 2 is due to formation of tin(IV) species,[40,43] as its intensity was found increase at the expense of the other two peaks upon bubbling air through the solution. This band is very intense and it causes therefore significant variations in the Raman spectra even if only a few percent of tin(II) is oxidised to tin(IV). This is unfortunately inevitable during manipulating the solutions and collection the spectra. Raman spectra of a more extended series of solutions with varying composition were also recorded; the obtained spectral parameters are given in Table S1. The peak positions (σ) and widths (FWHH) show only minor variations with varying solution composition. The slight increase in σ with the increasing concentration of the base is at the edge of significance (4–6 cm^{-1}). It is most probably associated with formation of contact ion-pairs, as variations of Raman shifts of this magnitude have been interpreted for other concentrated electrolyte systems in terms of contact ion-pair formation.[7,44,45] The Raman parameters obtained in media containing potassium instead of sodium are practically identical. The height is roughly linearly proportional to the total concentration of tin(II), Figure S1. These observations suggest, that there is only one tin(II)-containing species present in these solutions, the composition and structure of which is independent of the concentration of the solutes.

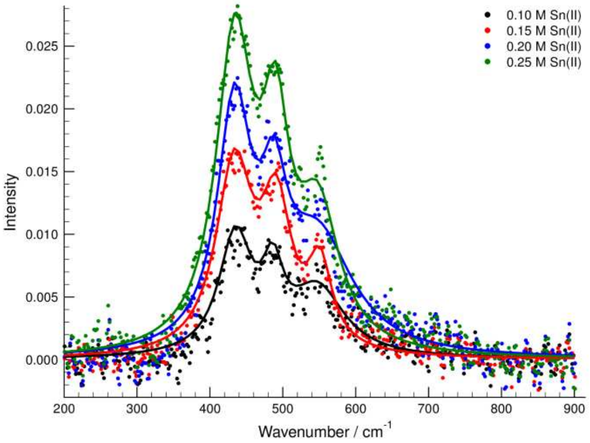

Fig. 2. The experimental (markers) and the fitted (lines) Raman spectra of the alkaline solutions with varying $C_{\mathrm{Sn(II)}}$ at $C_{\mathrm{NaOH}} = 4$ M.

Mössbauer spectroscopy

The ^{119}Sn Mössbauer spectrum consists of a slightly asymmetric doublet, Figure 3. The typical isomer shift and quadrupole splitting are $\delta = 2.58$ mm/s and $\Delta = 2.06$ mm/s, respectively. These Mössbauer parameters are in the range of those found for $Sn(OH)_2$ (δ = 2.3 - 2.95 mm/s and Δ = 2.13 - 3.05 mm/s)[46,47] as well as for SnO (δ = 2.6 – 3.4 mm/s and Δ = 1.3 – 2.28 mm/s) as reported in the literature.[48-51] The Mössbauer spectra reflect that tin is present in a single microenvironment solely as tin(II) in hyper-alkaline aqueous solution. This micro environment can be associated with the $[Sn(OH)_3]^-$ complex having trigonal pyramiddal geometry. No significant change was found in the Mössbauer parameters of this doublet when the concentration of tin(II) or NaOH was changed, Table S2. Since the hyperfine interactions detected by the Mössbauer spectroscopy are mostly affected by the first coordination sphere of tin, mainly the effect of oxygen nearest neighbour environment of tin(II) can be detected in the alkaline solutions, which remains unchanged with changing solution composition. The Δ values were calculated according to literature procedures[34] for $[Sn(OH)_3]^-$ and $[SnO(OH)]^-$. It was found, that the calculated Δ value for the $[SnO(OH)]^-$ complex was much larger (3.11 mm/s) than the experimentally observed one. The calculated Δ value for $[Sn(OH)_3]^-$ was 2.62 mm/s. The δ (2.72 mm/s) and Δ (2.26) values[50] obtained for the solid $NaSn(OH)_3$ are also close to those found in this study, however, the local structure of tin(II) in this compound is not established. Based on the analogy between F^- and OH^-, it is remarkable, that the Δ values for the $MSnF_3$ compounds (M = Na, K, Rb and Cs)[53] are in the range of 1.84 – 2.00 mm/s, while Δ = 2.15 mm/s for SnF_2;[54] tin(II) has trigonal pyramidal configuration in solid SnF_2.[55]

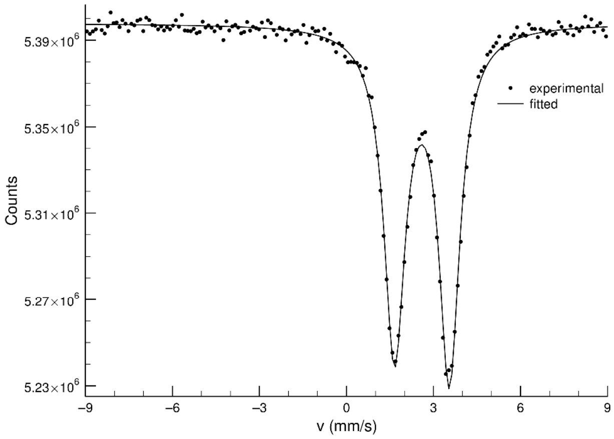

Fig. 3. ^{119}Sn Mössbauer spectrum of a representative frozen solution with $C_{\mathrm{Sn(II)}} = 0.2$ mol·dm^{-3} and $C_{\mathrm{NaOH}} = 4$ mol·dm^{-3}, (T = 20 K).

^{117}Sn NMR spectroscopy

The ^{117}Sn NMR spectrum of a solution containing 0.1 mol·dm^{-3} $SnCl_2$ and 4 mol·dm^{-3} NaOH consist of a quite sharp singlet peak at 727 ppm relative to the also singlet peak of a solution of 0.5 mol·dm^{-3} $Sn(ClO_4)_2$ in 1 mol·dm^{-3} $HClO_4$. This can be related to a single species, which is in complete agreement with the previous observations. The exchange of the water molecules for hydroxide ions binding to tin causes a large up-field shift. The chemical shift did not change within the experimental error when the tin(II) or the hydroxide concentration was varied.

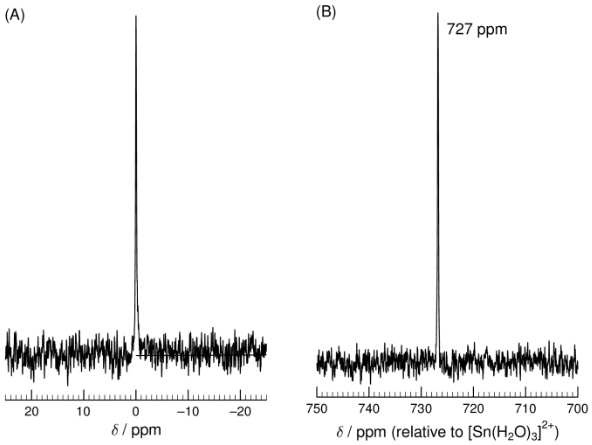

Fig. 4. (A) The ^{117}Sn NMR spectrum of a solution containing 0.5 mol·dm^{-3} $Sn(ClO_4)_2$ and 1 mol·dm^{-3} $HClO_4$ 0.1 mol·dm^{-3} $SnCl_2$ (tin(II) present as $[Sn(H_2O)_3]^{2+}$), and (B) and 0.1 mol·dm^{-3} $SnCl_2$ in 4 mol·dm^{-3} NaOH (tin(II) present as $[Sn(OH)_3]^-$), the chemical shift is relative to the acidic sample (A).

Quantum chemical calculations

For *ab initio* calculations, a 3-legged stool like (trigonal pyramid) structure was assumed for the $[Sn(OH)_3]^-$ complex and a V-shaped arrangement for the $[SnO(OH)]^-$ complex; the O-Sn-O angle is assumed to be close to 90° in both cases. The primary Sn–O bond lengths were found to be 2.10 Å, and 1.98 and 2.13 Å for the three- and two coordinated complex, respectively. The

Raman spectra of these species have been calculated, Figure 5. In the calculated spectra of both species, peaks are seen at around 430 and 490 cm^{-1}, with larger intensity corresponding to the band at the lower wavenumber, which is in excellent agreement with the experimental spectra, Figure 2. The striking difference is, that the most intense calculated peak, corresponding to $[SnO(OH)]^-$, is found at 700 cm^{-1}, which is completely missing in the experimental spectra (Figure 2), strongly suggesting that the observed spectra corresponds to the three-coordinated complex $[Sn(OH)_3]^-$.

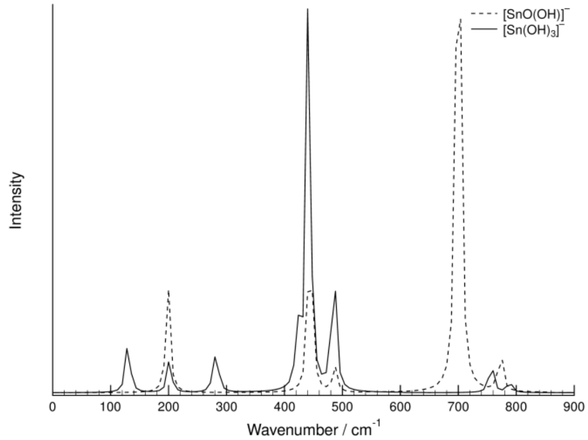

Fig. 5. Calculated Raman spectra of $[Sn(OH)_3]^-$ (solid line) and $[SnOOH]^-$ (dashed line).

X-ray absorption spectroscopy

The selection of an appropriate, non-interfering counter anion was the first step during the investigation. It is convenient to prepare tin(II) stock solutions using hydrochloric acid as the dissolution is rapid and the solubility of $SnCl_2$ is quite high due to the formation of chlorido complexes. The solubility of $Sn(ClO_4)_2$ is significantly lower than that of $SnCl_2$, and the dissolution of SnO or metallic tin is much slower in perchloric than in hydrochloric acid. It is therefore important to secure that tin(II)-chlorido complexes are not out-competing the tin(II)-hydroxido complexes in strong alkaline solution. As no literature data are available for the tin(II)-chloride system at pH > 13, X-ray absorption spectroscopy was applied to study whether tin(II)-chlorido or chlorido-hydroxido mixed complexes are formed under such conditions or not. XAS spectra of 0.1 mol·dm^{-3} $SnCl_2$ in 1 mol·dm^{-3} hydrochloric acid, in 4 mol· dm^{-3} NaOH, and in 4 mol·dm^{-3} NaOH + 1 mol·dm^{-3} NaCl, were compared with the spectra of 0.1 mol·dm^{-3} $Sn(ClO_4)_2$ in 1 mol·dm^{-3}perchloric acid and in 4 mol·dm^{-3} NaOH. The compositions of the alkaline tin(II) solutions prepared for the detailed study of the local structure are given in Table 1.

The X-ray absorption near-edge structure (XANES) regions and the Fourier-transform of the k^3-weighted extended X-ray absorption fine structure (EXAFS) data of the measured samples are presented on Figure 6 (A). As the figure shows, the spectra of the two acidic samples are clearly distinguishable in both the XANES region and the Fourier transform of the EXAFS region. In 1 mol·dm^{-3} hydrochloric acid tin(II) is almost exclusively present as $[SnCl_3]^-$ complexes,[56] and the fitting of the EXAFS data gave a mean Sn-Cl bond distance of 2.475(2) Å, a Debye-Waller factor coefficient (σ^2) of 0.0098(8) Å^2, and a coordination number (N) was set to 3, with an assumed trigonal pyramidal geometry, which is in good agreement with relevant crystal structures, Table S3; the fits of the EXAFS function and the Fourier transform are shown in Figure S2. In 1 mol·dm^{-3} perchloric acid tin(II) is present as hydrated tin(II) ions, $[Sn(H_2O)_3]^{2+}$,[2] where $N = 3$ (fixed parameter), $r = 2.178(5)$ Å and $\sigma^2 = 0.0153(4)$ Å^2. On the contrary, the spectra of the three alkaline samples are identical, even if a large excess of chloride ions (1 mol·dm^{-3}) is present. This shows clearly that the presence of chloride ions, also at high concentrations, has no effect on the tin(II) speciation as long as the free hydroxide concentration exceeds 0.1 mol·dm^{-3}. The chloride ion can therefore be considered as a truly non-interfering counter ion in the experiments performed on tin(II) in hyper-alkaline aqueous solution.

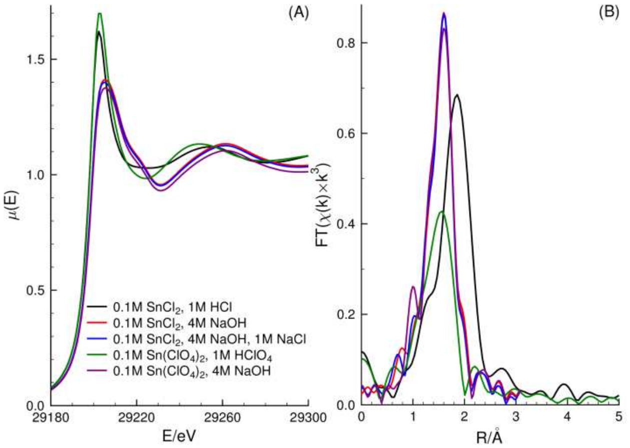

Fig. 6. The near-edge region of the Sn K-edge X-ray absorption spectra of 0.1 mol·dm^{-3} $SnCl_2$ in 1 mol·dm^{-3} hydrochloric acid, in 4 mol·dm^{-3}NaOH, and in 4 mol·dm^{-3}NaOH + 1 mol·dm^{-3}NaCl, compared to the spectra of 0.1 mol·dm^{-3} $Sn(ClO_4)_2$ in 1 mol·dm^{-3}perchloric acid and in 4 mol·dm^{-3} NaOH (A) and the Fourier-transform of the k^3-weighted EXAFS data of them (B)

The edge positions show that these samples contained exclusively tin(II), as the experimentally observed reference edge energy for tin(II) in solid SnO and for tin(IV) in solid SnO_2 was 29207.45 and 29211.45 eV, respectively, and the edge energy of the samples was found to be 29207.13 eV. Thus the experimental protocol employed during the experiments was suitable to protect the samples from aerial oxidation.

Cite this: DOI: 10.1039/c0xx00000x

www.rsc.org/xxxxxx

ARTICLE TYPE

Table 1 Composition of hyper-alkaline aqueous tin(II) samples studied, expressed in total molar concentrations, and the structure parameters in the refinements of the EXAFS data collected at ambient temperature using the EXAFSPAK program package, including number of Sn-O bond distances, *N*, mean Sn-O bond distance, *d*/Å, and Debye-Waller factor coefficient, σ^2/Å^2,the threshold energy, E_o/eV, the amplitude reduction factor the goodness, S_o^2, the goodness of fit, *F*/%, as expressed in the EXAFSPAK program package, ref. 38.

N=3	Sn10_2	Sn10_4	Sn10_8	Sn10_12	Sn5_4	Sn15_4	Sn20_4
C_{NaOH}	2	4	8	12	4	4	4
$C_{Sn(II)}$	0.1	0.1	0.1	0.1	0.05	0.15	0.20
R	2.079(5)	2.075(8)	2.075(3)	2.077(0)	2.076(2)	2.077(9)	2.076(4)
σ^2	0.0039(8)	0.0036(7)	0.0037(6)	0.0039(3)	0.0037(7)	0.0037(5)	0.0039(6)
E_o	29225.9(3)	29225.3(2)	29225.6(3)	29226.3(3)	29225.7(4)	29225.7(2)	29225.1(0)
S_o^2	1.20(6)	1.17(5)	1.17(7)	1.15(9)	1.17(8)	1.15(6)	1.19(5)
F	15.6	13.4	18.0	18.0	14.2	14.6	19.9

Structure determination of the [Sn(OH)$_3$]$^-$ complex in hyper-alkaline aqueous solution

By combining the information obtained by the potentiometric pH titrations, the FT-Raman, Mössbauer, ^{117}Sn NMR and K edge Sn XANES spectroscopy studies, and the quantum chemical calculation of Raman spectra of the [Sn(OH)$_3$]$^-$ and [SnOOH]$^-$ complexes it can be beyond any doubt be stated that one single tin(II) species is completely predominating in aqueous hyper-alkaline solution, [Sn(OH)$_3$]$^-$, independent of tin(II) concentration and free hydroxide concentrations above 0.1 mol·dm^{-3}. This is further evidenced by that all spectra of tin(II) in Figure 7 (A) are superimposable, and that the local structure of tin(II) in these hyper-alkaline solutions is identical and independent of the total concentration of both NaOH and tin(II) within the concentration range covered.

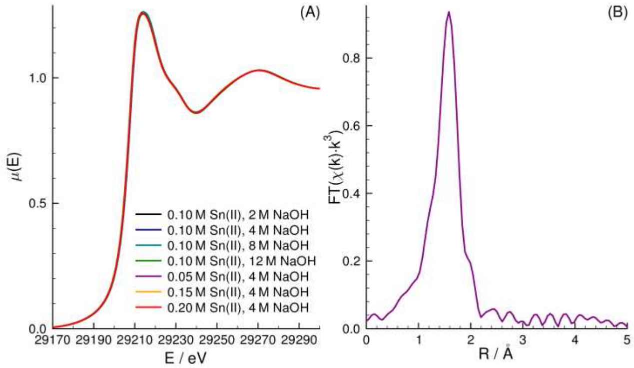

Fig. 7. The near-edge region of the alkaline Sn K-edge X-ray absorption spectra of all the alkaline solutions investigated: Sn10_2, Sn10_4, Sn10_8, Sn10_12, Sn5_4, Sn15_4, Sn20_4 (A) and the Fourier-transform of the k^3-weighted EXAFS data (B) of sample (Sn5_4). The acronyms used here are defined in Table 1.

The structure of the trihydroxidostannate(II), [Sn(OH)$_3$]$^-$, complex has been determined in the tin(II) and hydroxide concentration ranges 0.05-0.20 and 2-12 mol·dm^{-3}, respectively. In the following details will only be given for solution containing 0.05 mol·dm^{-3} tin(II) in 4 mol·dm^{-3} NaOH (Sn5_4), while data for the remaining solutions are given in Table 1.

The Fourier transform of the k^3-weighted EXAFS spectrum is given in Figure 7 (B). This Fourier transform has only a single peak related to the primary Sn-O bond distance at ~2.1 Å (~1.6 Å, not phase corrected). According to this single peak, tin(II) is expected to have a simple local environment, and no multiple scattering from the atoms in the first coordination sphere was detected. This indicates low symmetry around tin(II) as expected from the trigonal pyramidal configuration of three-coordinated tin(II) complexes, Table S3. Polynuclear tin(II) complexes have not been detected under these conditions as no Sn···Sn pair-interactions are seen on Fourier-transform of the k^3-weighted EXAFS data. Bond lengths are more accurately determined by EXAFS than the corresponding coordination numbers,[55] but as the other spectroscopic methods applied in this study clearly shows the presence of only the trihydroxidostannate(II) complex the coordination number has been locked to three in all refinements.

The relationship between bond distance and coordination number can therefore in most cases be used to accurately estimate the coordination number from the observed bond distance.[58,59] The r_{Sn-O} and *N* values of solid O-coordinated tin(II) compounds were collected from the Inorganic Crystal Structure Database and the Cambridge Crystal Structure Database,[60,61] as previously done for lead(II);[62] the data are given as supplementary information, Table S4. The r_{M-O} *vs.* *N* data collected for both metal ions are shown on Figure 8. It is of utmost importance to stress that the spread in the Sn-O bond distances for complexes with the same coordination number and geometry is unusually large, and this is in particular the case for $N = 3$; the Sn-O bond lengths are in the range 2.066-2.185 Å. This is most likely due to the stereochemical impact of the occupied anti-bonding orbitals of tin(II), and the energy difference between occupied bonding and anti-bonding orbitals for different ligands. It shall also be mentioned that a mean Sn-O bond distance of 2.080 Å in the [Sn(OH)$_3$]$^-$ unit in the solid state has been reported.[63]

The [Sn(OH)$_3$]$^-$ complex is assumed to have trigonal pyramidal geometry, with the tin(II) on the top of the pyramid as found for the $[Sn(OH)_3]^-$ complex in the solid state[63] and of other three-coordinate tin(II) complexes, Table S3. During the fitting of the EXAFS data, N was held constant ($N = 3$), and a short bond length, $r_{Sn\text{-}O} = 2.076$ Å, as well as a small Debye-Waller factor, $\sigma^2 = 0.0038$ Å^2, were obtained, Table 1.

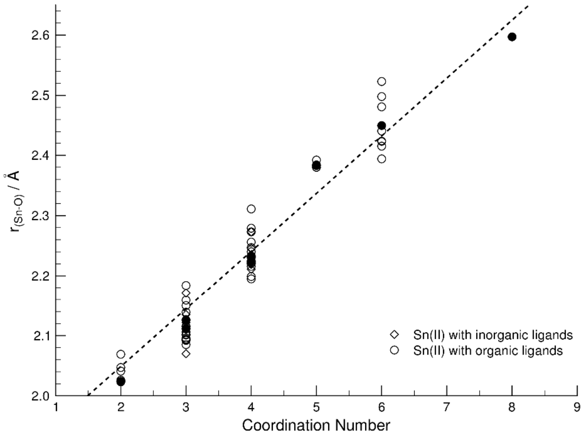

Fig 8. Summary of mean bond distances in tin(II) and compounds (details in Table S4, and the relationship between the Sn-O bond lengths and the coordination number in various O-coordinated tin(II) compounds. The filled symbols stand for the average values. The dashed line represents the linear trend-line of the mean M-O bond distances as function of coordination number.

Conclusions

The Sn(II):OH^- ratio is unambiguously determined to 1:3 in hyper-alkaline aqueous solution from potentiometric titrations using H_2/Pt electrode and Raman, Mössbauer and Sn K edge XANES spectroscopic studies and *ab initio* quantum chemical calculations, and that the trihydroxidostannate(II) complex, $[Sn(OH)_3]^-$, is exclusive, or at least overwhelmingly predominant, tin(II) species in hyper-alkaline aqueous solution. The structure of the $[Sn(OH)_3]^-$ complex is most likely trigonal pyramidal (3-legged stool) as all three-coordinate tin(II) complexes reported in the solid state, Table S3. The Sn-O bond length in the $[Sn(OH)_3]^-$ complex has been determined by EXAFS to 2.078 Å, which is on the short side but within the range of bond distances observed for tin(II) complexes coordinated by three oxygens, while in the $[Sn(H_2O)_3]^{2+}$ it is on the long side, 1.178 Å. This shows that Sn-O bond distance vary remarkably much within the same coordination number for different kind of oxygen donor ligands. The presence of chloride ions, even in high concentrations, has no effect on the speciation of the hydroxidostannte(II) complexation in hyper-alkaline aqueous solution as proven by the XAS measurements.

Acknowledgment

Research leading to this contribution was supported by the National Research Fund of Hungary through OTKA 83889 and TÁMOP-4.2.2.C-11/1KONV-2012-0010. The X-ray absorption measurements were supported by the CALIPSO (TNA, European Union) program. Éva G. Bajnóczi would like to thank the Campus Hungary Scholarship of the Balassi Institute which financed a five week short term study at the Department of Chemistry and Biotechnology, Swedish University of Agricultural Sciences, Uppsala, Sweden. Great thanks to Valérie Briois, beam-line scientist at SAMBA, Soleil, for her essential help during the X-ray absorption measurements.

Notes and references

[a] *Department of Inorganic and Analytical Chemistry, University of Szeged, H-6720 Dóm tér 7., Szeged, Hungary*
[b] *Laboratory of Nuclear Chemistry, Institute of Chemistry, Eötvös Loránd University, Pázmány Péter sétány 1/A, Budapest H-1117, Hungary*
[c] *Institute of Molecular Pharmacology, Research Centre for Natural Sciences, HungarianAcademy of Sciences, Magyar tudósok körútja 2., H-1117 Budapest, Hungary*
[d] *Institute of Pharmaceutical Analysis, University of Szeged, Somogyi u. 4, Szeged H-6720, Hungary*
[e] *Department of Physical Chemistry and Materials Science, University of Szeged, H-6720 Aradi vértanúk tere 1., Szeged, Hungary*
[f] *Department of Organic Chemistry, University of Szeged, H-6720 Dóm tér 8., Szeged, Hungary*
[g] *Department of Chemistry and Biotechnology, Swedish University of Agricultural Sciences, P.O.Box 7015, SE-750 07, Uppsala, Sweden*
[h] *Materials and Solution Structure Research Group, Institute of Chemistry, University of Szeged H-6720 Aradi vértanúk tere 1., Szeged, Hungary*
[*] *Corresponding authors: sipos@chem.u-szeged.hu, Ingmar.persson@slu.se*

† Electronic Supplementary Information (ESI) available: summary of solid state structures of chlorostannate(II) and oxygen coordinated tin(II) complexes reported in the literature, Raman and Mössbauer spectroscopic parameters of aqueous alkaline tin(II) solutions, fit of EXAFS data of the trichlorosatnnate(II) complex in water and integrated Raman intensities of the 430 cm^{-1} band in hyper-alkaline aqueous solutions. See DOI: 10.1039/b000000x/

1 A. Pallagi, É. G. Bajnóczi, S. E. Canton, T. B. Bolin, G. Peintler, B. Kutus, Z. Kele, I. Palinko and P. Sipos, *Env. Sci. Technol.*, 2014, **48,** 6604-6611.
2 A. Pallagi, Á. G. Tasi, G. Peintler, P. Forgo, I. Palinko and P.Sipos, *Dalton Trans.*, 2013, **42,** 13470-13476.
3 E. Horváth, Á. Kukovecz, Z. Kónya and I. Kiricsi, *Chem. Mater.*, 2007, **4**, 927-931.
4 D. Srankó, A. Pallagi, E. Kuzmann, S. E. Canton, M. Walczak, A. Sápi, A. Kukovecz, Z. Kónya,P. Sipos and I. Palinko, *Appl. Clay Sci.*, 2010, **48,** 214-217.
5 A. E. Martell; R. M. Smith, Critical Stability Constants; Plenum Press: London , 1975.
6 F. Baes, R. E. Mesmer, The Hydrolysis of Cations, John Wiley & Sons: NewYork, 1976; Ch. 15.3.
7 P. Sipos, *J. Mol. Liq.*, 2010, **146**, 1-14.
8 P. Sipos, P. M. May and G. Hefter, *Dalton Trans.*, 2006, 368-375
9 R. Buchner, P. Sipos,G. Hefter and P. M. May, *J. Phys. Chem. A*, 2002, **106,** 6527-6532.
10 P. Sipos, T. Megyes and O. Berkesi, *J. Soln. Chem.* 2008, **34,** 1411-1418.
11 T. Radnai, Sz. Bálint, I. Bakó, T. Megyes, T. Grósz, A. Pallagi, G. Peintler, I. Palinko and P. Sipos, *Phys. Chem. Chem Phys.* 2014, **16,** 4023-4032.
12 N. Tarapova, A. Radkevich, D. Davydov, A. Titov and I. Persson, *Inorg. Chem.,* 2009, **48,** 10383-10388.
13 B. Zydorczak, P. M. May, D. P. Meyrick, D. Batka and G. T. Hefter, *Ind. Eng. Chem. Res.* 2012, **51,** 16537-16543.
14 N. Perera, G. T. Hefter and P. Sipos, *Inorg. Chem.* 2001, **40,** 3974-3978.
15 P. Sipos, S. G. Capewell, P. M. May. G. T. Hefter, G. Laurenczy, F. Lukács and R. Roulet, *J. Solution Chem.* 1997, **26**, 419-431.

16 P. Sipos, S. G. Capewell, P. M. May. G. T. Hefter, G. Laurenczy, F. Lukács and R. Roulet, *J. Chem. Soc., Dalton Trans.* 1998, 3007-3012.

17 M. Navarro, P. M. May, G. Hefter and E. Königsberger, *Hydrometallurgy* 2014,**147-148,** 68-72.

18 P. Sipos, D. Zeller, E. Kuzmann, A. Vértes, Z. Homonnay, M. Walczak and S. Canton, *Dalton Trans.* 2008, 5603-5611.

19 M. Altmaier, X. Gaona and T. Fenghanel, *Chem. Rev.* 2013, **113,** 901-943.

20 R. M. Cigala, F. Crea, C. De Stefano, G. Lando, D. Milea and S. Sammartano, *Geochim. Cosmochim. Acta*, 2012, **87**, 1-20.

21 F. Séby, M. Potin-Gautier, E. Giffaut and O. F. X. Donard, *Geochim. Cosmochim. Acta*, 2001, **65**, 3041-3053.

22 H. Gamsjäger, T. Gajda, J. Sangster, S. K. Saxena and W Voigt, *Chemical Thermodynamics*; ed. J. Perrone, OECD Publishing: 2012; vol 12, ch 7.

23 W. Mark, *Acta Chem. Scand., Ser. A* 1977, **31,** 157-162.

24 F. A. Cotton and G. Wilkinson, *Advanced Inorganic Chemistry*, Wiley Interscience, New York, USA, 1988, p. 296.

25 P. Sipos, G. T. Hefter and P. M. May*, J. Chem. Eng. Data* 2000, **45**, 613-616.

26 P. Sipos, G. T. Hefter and P. M. May, *The Analyst*, 2000, **125,** 955-958.

27 P. Sipos, G. T. Hefter and P. M. May, *Aust. J. Chem*. 1998, **51,** 445-454.

28 P. Sipos, M. Schibeci, G. Peintler, P. M. May and G. T. Hefter, *Dalton Trans*. 2006, 1858-1866.

29 F. Menges "Spekwin32 - optical spectroscopy software", Version 1.71.6.1, 201x, http://www.effemm2.de/spekwin/ (accessed August 2014)

30 http://www.qtiplot.com/index.html (accessed August 2014)

31 Z. Klencsár, E. Kuzmann and A. Vértes, *J. Radioanal. Nucl. Chem.* 1996, **201,** 105-118.

32 http://www.medc.dicp.ac.cn/index.php (accessed August 2014)

33 Gaussian 09, Revision D.01, M. J. Frisch, G. W. Trucks, H. B. Schlegel, G. E. Scuseria, M. A. Robb, J. R. Cheeseman, G. Scalmani, V. Barone, B. Mennucci, G. A. Petersson, H. Nakatsuji, M. Caricato, X. Li, H. P. Hratchian, A. F. Izmaylov, J. Bloino, G. Zheng, J. L. Sonnenberg, M. Hada, M. Ehara, K. Toyota, R. Fukuda, J. Hasegawa, M. Ishida, T. Nakajima, Y. Honda, O. Kitao, H. Nakai, T. Vreven, J. A. Montgomery, Jr., J. E. Peralta, F. Ogliaro, M. Bearpark, J. J. Heyd, E. Brothers, K. N. Kudin, V. N. Staroverov, R. Kobayashi, J. Normand, K. Raghavachari, A. Rendell, J. C. Burant, S. S. Iyengar, J. Tomasi, M. Cossi, N. Rega, J. M. Millam, M. Klene, J. E. Knox, J. B. Cross, V. Bakken, C. Adamo, J. Jaramillo, R. Gomperts, R. E. Stratmann, O. Yazyev, A. J. Austin, R. Cammi, C. Pomelli, J. W. Ochterski, R. L. Martin, K. Morokuma, V. G. Zakrzewski, G. A. Voth, P. Salvador, J. J. Dannenberg, S. Dapprich, A. D. Daniels, Ö. Farkas, J. B. Foresman, J. V. Ortiz, J. Cioslowski and D. J. Fox, Gaussian, Inc., Wallingford CT, 2009.

34 G. Barone, A. Silvestri, G. Ruisi and G. L. Manna, *Chem. Eur. J.*, 2005, **11**, 6185-6191

35 S. Kárpáti, R. Szalay, A. G. Császár, K. Süvegh and S. Nagy, *J. Phys. Chem. A*, 2007, **111**, 13172-13181;

36 J. W. Krogh, G. Barone and R. Lindh, *Chem. Eur. J.*, 2006, **12**, 5116-5121

37 A. Thompson, D. Attwood, E. Gullikson, M. Howells, K-J. Kim, J. Kirz, J. Kortright, I. Lindau, Y. Liu, P. Pianetta, A. Robinson, J. Scofield, J. Underwood, G. Williams and H. Winick, X-ray data booklet, Lawrence Berkley National Laboratory, 2009.

38 G. N. George and I. F. Pickering, EXAFSPAK - A suite of Computer Programs for Analysis of X-ray absorption spectra, Stanford Synchrotron Radiation Laboratory, Stanford, CA, 1995. http://www-ssrl.slac.stanford.edu/exafspak.html (accessed August 2014)

39 S. I. Zabinsky, J. J. Rehr, A. Ankudinov, R. C. Albers and M. Eller*, Phys. Rev. B,* 1995, **52,** 2995-3009.

40 X. Huang, P. Tornatore and Y.-S- Li, *Electrochim. Acta*, 2000, **46**, 671-679.

41 M. Ocana, C. J. Serna and J. V. Garcia-Ramos, *Solid State Ionics*, 1993, **63,** 170-177.

42 J. C. Zou, C. Xu, X. Liu and C. Wang, *J. Appl. Phys.,* 1994, **75**, 1835-1836.

43 K. Nakamoto, Infrared and Raman Spectra of Inorganic and Coordination Compounds, John Wiley & Sons, New York, 1997.

44 I. Szilágyi, E. Königsberger and P. M. May, *Inorg. Chem.,* 2009, **48,** 2200-2204.

45 P. Sipos, L. Bolden, G. Hefter and P. M. May, *Aust. J. Chem.,* 2000, **53,** 887-890.

46 N. Alberola, *Polyhedron,* 1985, **4,** 1853-1857.

47 P. A. Flinn, Tin isomer shifts, In G.K. Shenoy and F.E. Wagner, Mössbauer Isomer Shifts, North Holland, Amsterdam, New York, Oxford, 1978

48 P. A. Cusack, P. J. Smith and W. J. Kroenke, *Polym. Degr. Stab.,* 1986, **14,** 307-318.

49 S. Ichiba and M. Takeshita, *Bull. Chem. Soc. Jpn.,* 1984, **57,** 1087-1091.

50 P. E. Lippens, *Phys. Rev. B,* 1999, **60,** 4576-4590.

51 P. S. Cook, J. D. Cashion and P. J. Cassidy, *Fuel,* 1985, **8,** 1121-1126.

52 W. Thornton and P. G. Harrison, *J. Chem. Soc., Faraday Trans.,* 1975, **71,** 461-472.

53 R. V. Paris, *Structure and Bonding in Tin Compounds*, in G. J. Long, Mössbauer Spectroscopy Applied to Inorganic Chemistry, Plenum Press, New York and London, 1984 and the references cited therein.

54 G. Ballard and T. Birchall, *Can. J. Chem.,* 1975, **53,** 3371-3373.

55 R. C. McDonald, H. H.-K. Hau and K. Eriks, *Inorg. Chem.,* 1976, **15,** 762-765.

56 M. Sherman, K. V. Ragnarsdottir, E. H. Oelkers and C. R. Collins, *Chem. Geol.* 2000, **167,** 169-176.

57 I. Persson, M. Sandström, H. Yokoyama and M. Chaudhry, *Z. Naturforsch., Sect. A.* 1995, **50,** 21-37.

58 R. D. Shannon, *Acta Crystallogr., Sect. A* 1976, **32,** 751-767.

59 D. Lundberg, I. Persson, L. Eriksson, P. D'Angelo and S. De Panfilis, *Inorg. Chem.* 2010, **49,** 4420-4432.

60 *Inorganic Crystal Structure Database*; FIZ Karlsruhe, 2013.

61 F. H. Allen, *Acta Crystallogr., Sect. B* 2002, **58,** 380-388.

62 I. Persson, K. Lyczko, D. Lundberg, L. Eriksson and A. Płaczek*, Inorg. Chem.*, 2011, **50,** 1058-1072, and references therein.

63 von H. G. Schnering, R. Nesper and H. Pelshenke, *Z. Anorg. Allg. Chem.* 1983, **499,** 117-129.